Performance Analysis of Mobile Edge Computing Network Applied Uplink NOMA with RF Energy Harvesting

Van-Truong Truong[1,2(✉)], Minh-Thong Vo[1,2], and Dac-Binh Ha[1,2]

[1] Faculty of Electrical-Electronic Engineering, School of Engineering and Technologies, Duy Tan University, Da Nang 550000, Vietnam
{truongvantruong,vominhthong}@dtu.edu.vn

[2] Institute of Research and Development, Duy Tan University, Da Nang 550000, Vietnam
hadacbinh@duytan.edu.vn

Abstract. In this paper, we study a mobile edge computing (MEC) network based on uplink non-orthogonal multiple access (NOMA) scheme with radio frequency energy harvesting (RF EH). Due to the energy and compute resources constraint, two users cannot complete their tasks by themselves within the maximum time delay. Therefore, they harvest the RF energy from a nearby access point (AP) and use all that energy to offload their tasks to the AP. We derive the closed-form expressions of the successful computation probability (SCP) of the users to evaluate system performance. We propose a algorithm based on genetic algorithm (GA) that determines the system's optimal time switching ratio to achieve the maximum SCP, namely MSCP-GA. Furthermore, we consider the numerical results to thoroughly understand the impact of parameters such as transmit power, time switching ratio on the system performance. Monte Carlo simulation is used to confirm the validity of our analysis.

Keywords: Mobile edge computing · Non-orthogonal multiple access · Uplink NOMA · Successful computation probability · MEC server · Genetic algorithm · Optimization

1 Introduction

In recent years, the next generation of wireless technology, i.e., 5G, has overgrown with outstanding supports of extreme speeds and capacity [1]. Technological breakthroughs in 5G have paved the way for developing many high-bandwidth applications such as virtual reality, augmented reality, autonomous cars, mobile online games, massive connected Internet of Things (IoT) [2]. However, mobile devices (MD) are currently not keeping up with the demand from these computation-intensive and latency-critical applications. It encouraged the

N.-S. Vo et al. (Eds.): INISCOM 2021, LNICST 379, pp. 57–72, 2021.
https://doi.org/10.1007/978-3-030-77424-0_6

development of Mobile Edge Computing (MEC), with the idea of shifting computation and data storage servers closer to MD [3].

Many technologies and scenarios in the 5G pattern integrated with MEC, in which NOMA and RF EH are two critical enabling technologies that researchers are very interested in. Applying NOMA in the MEC network has many benefits, including supporting many users, reducing latency and system energy consumption [4–7].

Ye *et al*. proposed NOMA MEC network in [4], in which two users offload their tasks to a MEC server located access point (AP) to ensure system delay constraint. Authors have used the derivative approach to maximize system performance in terms of successful computation probability (SCP) with three schemes: complete local computation, partial computation offloading, and complete offloading. In [5], Fang *et al*. proposed a multi-user NOMA MEC network, in which M users are randomly distributed in a single cell and computed by a MEC server located at BS center cell. The authors examined the system over Rayleigh fading and perfect channel state information (pCSI) conditions. A bisection searching algorithm is used to solve the problem of minimizing task computation time. Ha *et al*. in [6] proposed a downlink NOMA MEC network with two MEC APs to assist computation for a limited energy user. The authors proposed an APS algorithm based on channel gain to enhance the system's security performance. All of the above studies confirm the advantages of adopting NOMA over OMA when operating under the same schemes.

Besides, integrating RF EH techniques in MEC networks will solve limited battery lifetime, unstable grid power supply, and low computing capability [8–11]. Min *et al*. in [8] investigated the RF EH IoT healthcare monitoring system based on MEC. Multiple sensors use their battery and RF energy to gather parameters like blood pressure and electrocardiograms. They can operate their tasks by themselves or receive computational help from the MEC server to make urgent recommendations. The reinforcement learning algorithm is proposed to use CSI information, input tasks, and computational resources to optimize the sensors' offloading strategy. In [9], the authors proposed the RF EH NOMA MEC network operated with a two-phase protocol: wireless power transfer phase and computation phase. Algorithms based on the iterative algorithm and an alternative optimization algorithm are proposed to solve the problem of maximizing the system's computational performance. Garcia *et al*. in [11] wireless-powered multi-user NOMA MEC system assisted by a power beacon (PB) and AP in the presence of an eavesdropper. Specifically, AP and PB broadcast the RF energy to M users. Then, the users simultaneously offload the tasks to the MEC server located at the AP using NOMA. The authors assume the AP has considerable computational resources, so they ignore the computation time here. A solution based on particle swarm optimization (PSO) is proposed to maximize the system secrecy computation efficiency (SCE).

In this study, we consider the RF EH NOMA MEC system over Rayleigh fading channel. The main contributions of our paper are as follows.

- We investigated the RF EH NOMA MEC over Rayleigh fading.
- We derived the closed-form expression of successful computation probability for this system. Furthermore, we provided numerical results to investigate the impact of the network parameters, i.e., transmit power, time switching ratio, the task length, bandwidth, to verify RF EH NOMA deployment's effectiveness in the MEC network.
- We proposed an optimization algorithm based on a genetic algorithm to find the optimal time switching so that the SCP is maximized. Simulation results show that our proposed algorithm can improve the SCP.

The rest of this paper is organized as follows. Section 2 presents the system model. The performance of this considered system is analyzed in Sect. 3. We present the optimization problem in term of SCP in Sect. 4. The numerical results and discussion are shown in Sect. 5. Finally, we conclude our work in Sect. 6.

2 System Model

The system model for an uplink NOMA mobile edge computing network with energy harvesting is depicted as Fig. 1, in which two energy-constrained users (i.e., U_1 and U_2) offload their tasks to MEC access point (AP) through uplink NOMA by using the harvetsed energy from AP. All devices are assumed to have a single antenna and operate in the half-duplex mode. Assuming that U_1 and U_2 have L_1-bit and L_2-bit tasks, respectively, to be executed and they may not be able to execute their tasks locally within the latency budget due to the limited computational ability. Therefore, U_1 and U_2 offload their tasks to AP's server through wireless links subject to quasi-static Rayleigh fading. However, due to energy constraint, before transmission, U_1 and U_2 harvest the RF energy from AP and use this for offloading.

We propose a new protocol, called RF EH Uplink NOMA MEC scheme, for MEC network as follows.

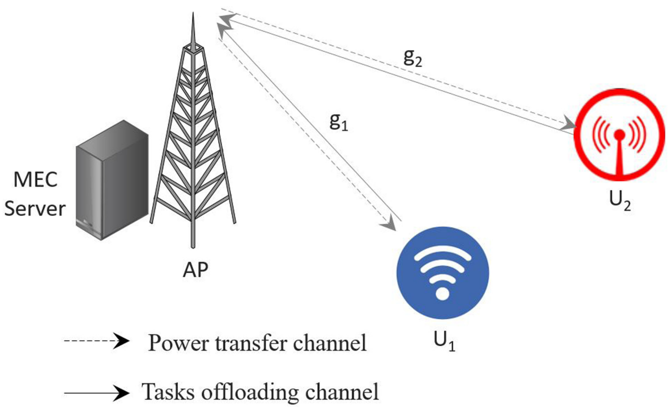

Fig. 1. System model for uplink NOMA MEC using RF EH network

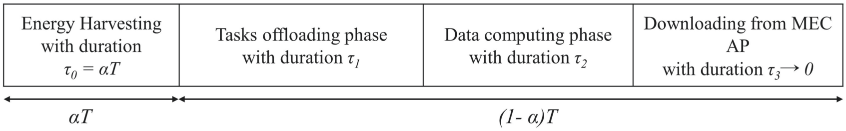

Fig. 2. Time flow chart for proposed system

- In the first phase (energy harvesting phase), the users harvest energy from AP during the duration of $\tau_0 = \alpha T$, where α denotes the time switching ratio, i.e., $0 < \alpha < 1$, and T stands for transmission block time. During this energy harvesting phase, the harvested energy of U_i, $(i \in (1, 2))$ is obtained by

$$E_i = \eta P_0 g_i \alpha T, \tag{1}$$

where $0 < \eta \leq 1$ stands for the energy conversion efficiency of the energy receiver [12], P_0 denotes the transmit power of AP, g_i denotes the channel power gain of link $\mathrm{U}_i - \mathrm{AP}$.

- In the second phase (offloading phase), U_i apply uplink NOMA scheme to offload their tasks to the AP's server during duration τ_1. On the basis of the principle of NOMA, the received signal of offloading tasks at MEC server is expressed as

$$y_{MEC} = h_1 \sqrt{P_1} x_1 + h_2 \sqrt{P_2} x_2 + n_{MEC}, \tag{2}$$

where h_i denotes the channel coefficient, x_i stands for the offloading task of the i^{th} user, $, i \in \{1, 2\}$. $n_{MEC} \sim \mathcal{CN}(0, \sigma^2)$ represents the AWGN at the MEC server. Note that $g_i = |h_i|^2$. The transmit power P_i calculated as follows

$$P_i = \frac{E_i}{(1-\alpha)T - \tau} = a P_0 g_i, \tag{3}$$

where $a \triangleq \frac{\eta \alpha T}{(1-\alpha)T - \tau}$. τ stands for the computing time at MEC server defined as follows:

$$\tau = \frac{\rho(L_1 + L_2)}{f}, \tag{4}$$

where ρ and f denote the number of required CPU cycles for each bit and the CPU-cycle frequency of MEC server, respectively.

- In the third phase (computing phase), according to the principle of uplink NOMA, AP first decodes the task x_i with larger power level by treating the remain with smaller power level as noise and then subtracts this component in duration τ_2. Hence, the signal-to-interference-plus-noise ratio (SINR) and the signal-to-noise ratio (SNR) for the MEC server to decode x_i are written as

if $g_1 > g_2$:

$$\gamma_{11} = \frac{a \gamma_0 g_1^2}{a \gamma_0 g_2^2 + 1}, \tag{5}$$

$$\gamma_{12} = a \gamma_0 g_2^2, \tag{6}$$

else

$$\gamma_{22} = \frac{a\gamma_0 g_2^2}{a\gamma_0 g_1^2 + 1}, \tag{7}$$

$$\gamma_{21} = a\gamma_0 g_1^2, \tag{8}$$

where $\gamma_0 = \frac{P_0}{\sigma^2}$. Then, these tasks are executed on the MEC server in duration τ_3.

- Finally, in the last phase (result returning phase), U_i downloads the results from AP during τ_3.

The time flow chart for EH Uplink-NOMA MEC protocol is as Fig. 2, in which τ_3 is assumed very small compared to transmission time and thus is neglected [4,7,13].

The i.i.d. quasi-static Rayleigh channel gains g_i, $i \in \{1, 2\}$, follows exponential distributions with parameters λ_i. Therefore, the cummulative density function (CDF) and probability density function (PDF) of g_i are respectively given by

$$F_{g_i}(x) = 1 - e^{-\frac{x}{\lambda_i}}, \tag{9}$$

$$f_{g_i}(x) = \frac{1}{\lambda_i} e^{-\frac{x}{\lambda_i}}. \tag{10}$$

3 Performance Analysis

In order to characterize the performance of a NOMA-MEC system, the successful computation probability, namely $\boldsymbol{\Phi_s}$, is used as an important performance metric [4,6,7]. It is defined as the probability that all tasks are successfully executed within a given time $T > 0$, which is expressed as

$$\boldsymbol{\Phi_s} = \Pr\left(\max\{t_1, t_2\} + \tau \leq (1-\alpha)T\right), \tag{11}$$

where t_1 and t_2 are the transmission latency of U_1 and U_2, respectively and calculated as follows:

$$\begin{cases} t_1 = \frac{L_1}{(1-\alpha)B\log(1+\gamma_{11})}, t_2 = \frac{L_2}{(1-\alpha)B\log(1+\gamma_{12})}, & g_1 > g_2 \\ t_1 = \frac{L_1}{(1-\alpha)B\log(1+\gamma_{21})}, t_2 = \frac{L_2}{(1-\alpha)B\log(1+\gamma_{22})}, & g_1 < g_2 \end{cases} \tag{12}$$

where B denotes the channel bandwidth.

In order to evaluate the performance of this considered NOMA MEC system, we obtain the following lemmas.

Lemma 1
Under quasi-static Rayleigh fading, the closed-form expression of the SCP $\Phi_s^{U_1}$ for this considered uplink RF EH NOMA MEC system is given by

$$\Phi_s^{U_1} = \begin{cases} \frac{\pi}{N\lambda_2}\sum_{j=1}^{N}\exp\left(-\frac{\sqrt{\gamma_{th1}\left(\theta_j^2+\frac{1}{a\gamma_0}\right)}}{\lambda_1}-\frac{\theta_j}{\lambda_2}\right)\sqrt{\frac{1-\phi_j}{1+\phi_j}} \\ +\frac{\lambda_2}{\lambda_1+\lambda_2}\exp\left[-\left(\frac{1}{\lambda_1}+\frac{1}{\lambda_2}\right)\sqrt{\frac{\gamma_{th1}}{a\gamma_0}}\right], & \gamma_{th1}>1 \\ \frac{\pi c}{2N\lambda_2}\sum_{j=1}^{N}\exp\left(-\frac{\sqrt{\gamma_{th1}\left(x_j^2+\frac{1}{a\gamma_0}\right)}}{\lambda_1}-\frac{x_j}{\lambda_2}\right)\sqrt{1-\phi_j^2} \\ +\frac{\lambda_1}{\lambda_1+\lambda_2}\exp\left[-\left(\frac{1}{\lambda_1}+\frac{1}{\lambda_2}\right)c\right]+\frac{\lambda_2}{\lambda_1+\lambda_2}\exp\left[-\left(\frac{1}{\lambda_1}+\frac{1}{\lambda_2}\right)\sqrt{\frac{\gamma_{th1}}{a\gamma_0}}\right], & \gamma_{th1}<1 \end{cases} \tag{13}$$

where $\gamma_{th1} = 2^{\frac{L_1}{\Omega_1(1-\alpha)B}} - 1$, $\Omega_1 = (1-\alpha)T - \frac{\rho L_1}{f}$, $c = \sqrt{\frac{\gamma_{th1}}{a\gamma_0(1-\gamma_{th1})}}$, $\theta_j = -\ln\left(\frac{\phi_j+1}{2}\right)$, $x_j = \frac{(\phi_j+1)c}{2}$, $\phi_j = \cos\left(\frac{2j-1}{2N}\pi\right)$, and N is the complexity-vs-accuracy trade-off coefficient.

Proof. See Appendix A.

Lemma 2
Under quasi-static Rayleigh fading, the closed-form expression of the SCP $\Phi_s^{U_2}$ for this considered uplink RF EH NOMA MEC system is given by

$$\Phi_s^{U_2} = \begin{cases} \frac{\pi}{N\lambda_1}\sum_{j=1}^{N}\exp\left(-\frac{\sqrt{\gamma_{th2}\left(\theta_j^2+\frac{1}{a\gamma_0}\right)}}{\lambda_2}-\frac{\theta_j}{\lambda_1}\right)\sqrt{\frac{1-\phi_j}{1+\phi_j}} \\ +\frac{\lambda_1}{\lambda_1+\lambda_2}\exp\left[-\left(\frac{1}{\lambda_1}+\frac{1}{\lambda_2}\right)\sqrt{\frac{\gamma_{th2}}{a\gamma_0}}\right], & \gamma_{th2}>1 \\ \frac{\pi c}{2N\lambda_1}\sum_{j=1}^{N}\exp\left(-\frac{\sqrt{\gamma_{th2}\left(x_j^2+\frac{1}{a\gamma_0}\right)}}{\lambda_2}-\frac{x_j}{\lambda_1}\right)\sqrt{1-\phi_j^2} \\ +\frac{\lambda_2}{\lambda_1+\lambda_2}\exp\left[-\left(\frac{1}{\lambda_1}+\frac{1}{\lambda_2}\right)c\right]+\frac{\lambda_1}{\lambda_1+\lambda_2}\exp\left[-\left(\frac{1}{\lambda_1}+\frac{1}{\lambda_2}\right)\sqrt{\frac{\gamma_{th2}}{a\gamma_0}}\right], & \gamma_{th2}<1 \end{cases} \tag{14}$$

where $\gamma_{th2} = 2^{\frac{L_2}{\Omega_2(1-\alpha)B}} - 1$, $\Omega_2 = (1-\alpha)T - \frac{\rho L_2}{f}$, $c = \sqrt{\frac{\gamma_{th2}}{a\gamma_0(1-\gamma_{th2})}}$, $\theta_j = -\ln\left(\frac{\phi_j+1}{2}\right)$, $x_j = \frac{(\phi_j+1)c}{2}$, $\phi_j = \cos\left(\frac{2j-1}{2N}\pi\right)$, and N is the complexity-vs-accuracy trade-off coefficient.

Proof. The proof of Lemma 2 is similar to the proof of Lemma 1; see Appendix A.

Lemma 3
Under quasi-static Rayleigh fading, the closed-form expression of the SCP Φ_s for this considered uplink RF EH NOMA MEC system is given by

$$\Phi_s = \begin{cases} \frac{\pi}{N\lambda_2}\sum_{j=1}^{N}\exp\left(-\frac{\sqrt{\gamma_{th}\left(\theta_j^2+\frac{1}{a\gamma_0}\right)}}{\lambda_1}-\frac{\theta_j}{\lambda_2}\right)\sqrt{\frac{1-\phi_j}{1+\phi_j}} \\ -\frac{\pi b}{2N\lambda_2}\sum_{j=1}^{N}\exp\left(-\frac{\sqrt{\gamma_{th}\left(x_j^2+\frac{1}{a\gamma_0}\right)}}{\lambda_1}-\frac{x_j}{\lambda_2}\right)\sqrt{1-\phi_j^2}, \\ +\frac{\pi}{N\lambda_1}\sum_{j=1}^{N}\exp\left(-\frac{\sqrt{\gamma_{th}\left(\theta_j^2+\frac{1}{a\gamma_0}\right)}}{\lambda_2}-\frac{\theta_j}{\lambda_1}\right)\sqrt{\frac{1-\phi_j}{1+\phi_j}} \\ -\frac{\pi b}{2N\lambda_1}\sum_{j=1}^{N}\exp\left(-\frac{\sqrt{\gamma_{th}\left(x_j^2+\frac{1}{a\gamma_0}\right)}}{\lambda_2}-\frac{x_j}{\lambda_1}\right)\sqrt{1-\phi_j^2}, & \gamma_{th}>1 \\ \frac{\pi(c-b)}{2N\lambda_2}\sum_{j=1}^{N}\exp\left(-\frac{\sqrt{\gamma_{th}\left(y_j^2+\frac{1}{a\gamma_0}\right)}}{\lambda_1}-\frac{y_j}{\lambda_2}\right)\sqrt{1-\phi_j^2} \\ +\frac{\lambda_1}{\lambda_1+\lambda_2}\exp\left[-\left(\frac{1}{\lambda_1}+\frac{1}{\lambda_2}\right)c\right] \\ +\frac{\pi(c-b)}{2N\lambda_2}\sum_{j=1}^{N}\exp\left(-\frac{\sqrt{\gamma_{th}\left(y_j^2+\frac{1}{a\gamma_0}\right)}}{\lambda_1}-\frac{y_j}{\lambda_2}\right)\sqrt{1-\phi_j^2} \\ +\frac{\lambda_1}{\lambda_1+\lambda_2}\exp\left[-\left(\frac{1}{\lambda_1}+\frac{1}{\lambda_2}\right)c\right], & \gamma_{th}<1 \end{cases} \tag{15}$$

where $\gamma_{th} = 2^{\frac{L}{\Omega(1-\alpha)B}} - 1$, $\Omega = (1-\alpha)T - \frac{\rho L}{f}$, $b = \sqrt{\frac{\gamma_{th}}{a\gamma_0}}$, $c = \sqrt{\frac{\gamma_{th}}{a\gamma_0(1-\gamma_{th})}}$, $\theta_j = -\ln\left(\frac{\phi_j+1}{2}\right)$, $x_j = \frac{(\phi_j+1)c}{2}$, $y_j = \frac{(\phi_j+1)(c-b)}{2} + b$, $\phi_j = \cos\left(\frac{2j-1}{2N}\pi\right)$, and N is the complexity-vs-accuracy trade-off coefficient.

Proof. See Appendix B.

4 SCP Optimization Problem and Solution

Based on the proposed system above, maximal the successful computation probability problem (MSCP) of users are declared the following:

$$(\text{MSCP}) : \max_{\alpha}\ (\Phi_s) \tag{16a}$$

$$\text{subject to} : \max\{t_1, t_2\} + \tau \le (1-\alpha)T \tag{16b}$$

$$0 < \alpha < 1 \tag{16c}$$

where constraints (16b) ensure that all tasks are processed within the maximum allowed delay. Constraints (16c) describe the time switching ratio.

To solve the MSCP, we propose to use the genetic algorithm (GA), namely MSCP-GA, described in Algorithm 1. GA is classified in evolutionary algorithms, simulating biological evolution in nature and following Darwin's theory of evolution, [14,15]. In GA, each chromosome in the population is the problem solution. We initialized a population with 50 random individuals. We deploy the uniform crossovers for the population as follow:

$$\alpha \leftarrow \epsilon\alpha_{p1} + (1-\epsilon)\alpha_{p2} \tag{17}$$

where α is the offspring time switching ratio, α_{p1} and α_{p2} are parents, ϵ is the random number from 0 to 1 that determine how many of the genes needed from parents, $\epsilon \sim U(0,1)$.

We use the roulette wheel selection technique [14] for selecting the individual parents. That means the better the fitness value will have more opportunities to be selected for the crossover process. Next, the random mutation was used on the population as follow:

$$\alpha \leftarrow \alpha\mu\beta \tag{18}$$

where μ is mutation rate, and β is the same length as the chromosome, and the elements in it are randomly selected 0 and 1.

Finally, the new population is formed based on the best fitness value. We get an optimal time switching ratio when the algorithm reaches the maximum number of iterations.

Algorithm 1. Maximal the successful computation probability based on Genetic Algorithm (MSCP-GA)

procedure MSCP-GA(Φ_s)
  Input $N, P_s, f, \rho, B, T, L_1, L_2$
  Output α^*
  Initialize population size $nPop$, crossover rate χ, mutation rate μ, the maximum evolutionary generation $MaxIt$.
  while $i < MaxIt$ **do**
    Use the fitness function (15) to evaluate the population.
    Crossover using (17) and Mutation using (18).
    Selection new populations.
    i = i + 1
  end while
  Return α^*

In the next section, we discuss the proposed algorithm complexity. The Heap Sorting algorithm is used to order the population and to get the best solutions. The number of operations required for the selection process is $nPop\log(nPop)$. The number of operations required for crossover process and mutation process is $\xi\frac{nPop}{2}$ and $\mu.nPop$. Thus, the algorithm complexity of MSCP-GA is given by:

$$TC = MaxIt.(nPop.\log(nPop) + \xi.\frac{nPop}{2} + \mu.nPop) \tag{19}$$

5 Numerical Results and Discussion

In this section, we provide the numerical results in terms of successful computation probability Φ_s to reveal the impact of key system parameters to the system performance. The simulation parameters used in this work are provided in Table 1 [6,16].

Table 1. Simulation parameters

Parameters	Notation	Typical Values
Number of antennas of each device	N	1
Transmit power	P_s	0–30dB
CPU-cycle frequency of MEC server	f	1 GHz
The number of CPU cycles for each bit	ρ	10
Channel bandwidth	B	1 GHz
The threshold of latency	T	10 ms
The number of data bits of U_1	L_1	60 Kbits
The number of data bits of U_2	L_2	20 Kbits
The population size	$nPop$	50
Crossover rate	χ	0.6
Mutation rate	μ	0.001
The maximum evolutionary generation	$MaxIt$	50

The impact of average transmit SNR (γ_0) and time switching ratio (α) on system performance in terms of successful computation probability Φ_s is shown in Fig. 3, 4 and 5. It is easy to observe that both user's SCP increases as γ_0 increases. It demonstrates that increasing the transmit power can improve the system performance. Next, the effect of α is also clearly shown in the two pictures above. When increasing α from 0 to 1, the SCP tends to increase gradually, achieving its maximum value and gradually decreasing. It can be explained that when α increases, the users will have more time to harvest RF energy and use that plentiful energy in offloading tasks. However, when α gets closer to 1, users do not have enough time to offload their tasks, resulting in an SCP decrease. It also proves the existence of α^* makes the SCP reach maximum value.

Figure 6 depicts the impact of the length of task of U_1 and bandwidth on system performance. In this experiment, we gradually increase the U_1 task length while keeping the task length of U_2. We observed that the increase in the length of the task of U_1 reduces its performance. However, it contributes to improving the probability of successful computation for U_2. Another observation is that increasing the bandwidth can improve system performance. In the case of very high bandwidth, the task's length does not affect system performance much.

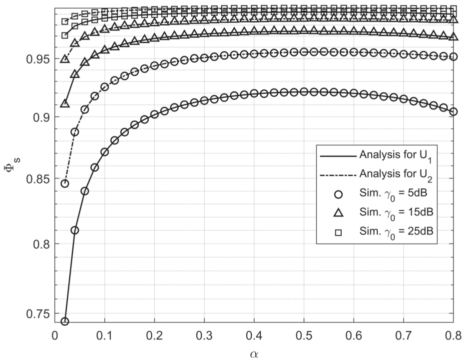

Fig. 3. $\Phi_s^{U_1}$ and $\Phi_s^{U_2}$ vs. time switching ratio α with different γ_0.

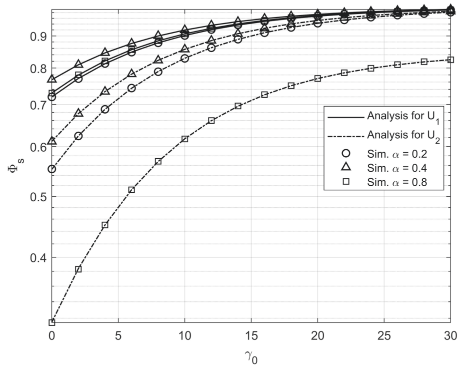

Fig. 4. $\Phi_s^{U_1}$ and $\Phi_s^{U_2}$ vs. average transmit SNR γ_0 with different α.

Figure 7 describes MSCP-GA rapidly converges with the setting parameters given in Table 1. Figure 8 describes comparison among the optimal algorithm and non-optimal approach in term of SCP. With the non-optimal approach, we use fixed time switching ratio, 0.1, 0.4 and 0.8, respectively, to evaluate system performance. The results show that the use of the MSCP-GA algorithm gives higher efficiency than not using the optimal algorithm. Furthermore, to highlight the advantages of MSCP-GA, we also compared it to the MSCP-based on brute force optimization (MSCP-BF) [17] case. The results show that two optimal algorithms give the same results. However, it should be noted that the algorithm complexity of MSCP-BF is higher than that of MSCP-GA. The results show that our proposed algorithm improves system performance.

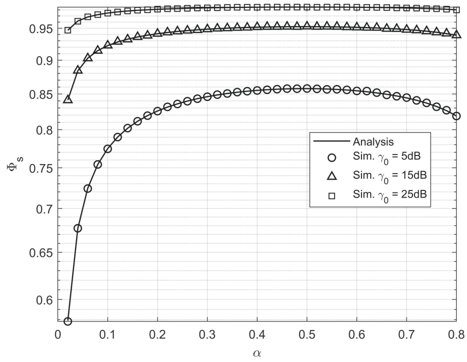

Fig. 5. Φ_s vs. time switching ratio α with different γ_0.

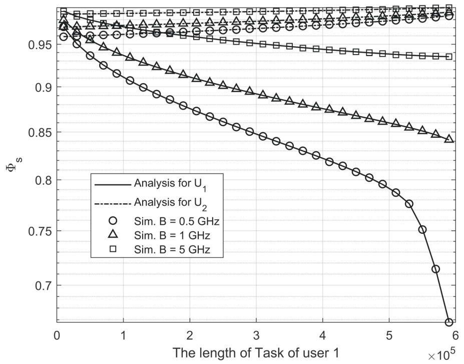

Fig. 6. Φ_s vs. the length of task of U_1 with different B.

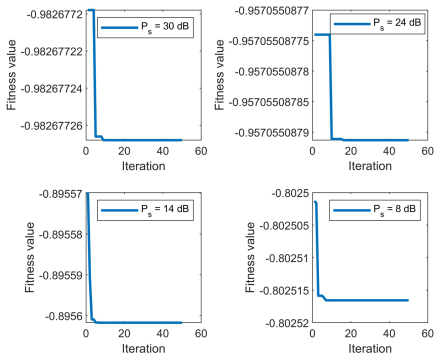

Fig. 7. Algorithm convergence when operating with different transmit power.

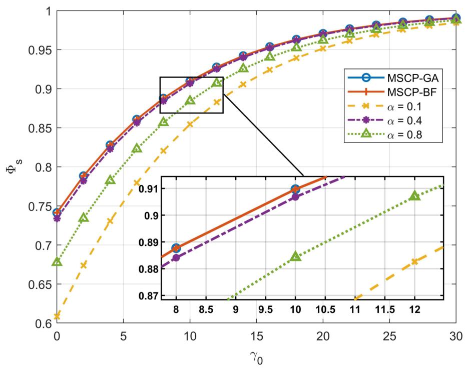

Fig. 8. System performance comparison among the optimal algorithm and non-optimal approach.

6 Conclusion

In this paper, we considered the uplink RF EH NOMA MEC network. Specifically, two energy-constraint users harvest RF energy from AP to offload their tasks. We derived the expression of the successful computation probability of two users and of system. We proposed a low-complexity approach based on the GA and achieved optimal system performance. Simulation results confirmed the superiority of the proposed algorithm in comparison with the traditional approach.

Appendix A: Proof of Lemma 1

Here, we derive the closed-form expression of $\varPhi_s^{U_1}$ as follows.

$$\begin{aligned}\varPhi_s^{U_1} &= \Pr\left(g_1 > g_2, \gamma_{11} > \gamma_{th1}\right) + \Pr\left(g_1 < g_2, \gamma_{21} > \gamma_{th1}\right)\\ &= \underbrace{\Pr\left(g_1 > g_2, \frac{a\gamma_0 g_1^2}{a\gamma_0 g_2^2 + 1} > \gamma_{th1}\right)}_{I_1} + \underbrace{\Pr\left(g_1 < g_2, a\gamma_0 g_1^2 > \gamma_{th1}\right)}_{I_2}\end{aligned} \quad \text{(A-1)}$$

$$
\begin{aligned}
I_1 &= \Pr\left(g_1 > g_2, g_1 > \sqrt{\gamma_{th1}\left(g_2^2 + \frac{1}{a\gamma_0}\right)}\right)\\
&= \begin{cases}
\Pr\left(g_1 > \sqrt{\gamma_{th1}\left(g_2^2 + \frac{1}{a\gamma_0}\right)}\right), & \gamma_{th1} > 1\\
\Pr\left(g_1 > \sqrt{\gamma_{th1}\left(g_2^2 + \frac{1}{a\gamma_0}\right)}, g_2 < \sqrt{\frac{\gamma_{th1}}{a\gamma_0(1-\gamma_{th1})}}\right) & \\
\qquad + \Pr\left(g_1 > g_2, g_2 > \sqrt{\frac{\gamma_{th1}}{a\gamma_0(1-\gamma_{th})}}\right), & \gamma_{th1} < 1
\end{cases}\\
&= \begin{cases}
\int_0^\infty \left[1 - F_{g_1}\left(\sqrt{\gamma_{th}\left(x^2 + \frac{1}{a\gamma_0}\right)}\right)\right] f_{g_2}(x)dx, & \gamma_{th} > 1\\
\int_0^c \left[1 - F_{g_1}\left(\sqrt{\gamma_{th}\left(x^2 + \frac{1}{a\gamma_0}\right)}\right)\right] f_{g_2}(x)dx & \\
\qquad + \int_c^\infty \left[1 - F_{g_1}(x)\right] f_{g_2}(x)dx, & \gamma_{th} < 1
\end{cases}
\end{aligned}
$$

$$
\overset{(a)}{=} \begin{cases}
\frac{\pi}{N\lambda_2}\sum_{j=1}^{N} \exp\left(-\frac{\sqrt{\gamma_{th}\left(\theta_j^2 + \frac{1}{a\gamma_0}\right)}}{\lambda_1} - \frac{\theta_j}{\lambda_2}\right)\sqrt{\frac{1-\phi_j}{1+\phi_j}}, & \gamma_{th} > 1\\
\frac{\pi c}{2N\lambda_2}\sum_{j=1}^{N} \exp\left(-\frac{\sqrt{\gamma_{th}\left(x_j^2 + \frac{1}{a\gamma_0}\right)}}{\lambda_1} - \frac{x_j}{\lambda_2}\right)\sqrt{1-\phi_j^2} & \\
\qquad + \frac{\lambda_1}{\lambda_1+\lambda_2}\exp\left[-\left(\frac{1}{\lambda_1} + \frac{1}{\lambda_2}\right)c\right], & \gamma_{th} < 1
\end{cases}. \tag{A-2}
$$

where $c = \sqrt{\frac{\gamma_{th}}{a\gamma_0(1-\gamma_{th})}}$, step (a) is obtained by applying the Gaussian-Chebyshev quadrature method [18] in which $\theta_j = -\ln\left(\frac{\phi_j+1}{2}\right)$, $x_j = \frac{(\phi_j+1)c}{2}$, $\phi_j = \cos\left(\frac{2j-1}{2N}\pi\right)$, and N is the complexity-vs-accuracy trade-off coefficient.

Next, we obtain the expression of integral I_2 as follows:

$$
\begin{aligned}
I_2 &= \Pr\left(\sqrt{\frac{\gamma_{th1}}{a\gamma_0}} < g_1 < g_2\right) = \int_{\sqrt{\frac{\gamma_{th1}}{a\gamma_0}}}^{\infty}\left[F_{g_1}(x) - F_{g_1}\left(\sqrt{\frac{\gamma_{th1}}{a\gamma_0}}\right)\right] f_{g_2}(x)dx\\
&= \frac{\lambda_2}{\lambda_1+\lambda_2}\exp\left[-\left(\frac{1}{\lambda_1} + \frac{1}{\lambda_2}\right)\sqrt{\frac{\gamma_{th1}}{a\gamma_0}}\right].
\end{aligned} \tag{A-3}
$$

From (A-1), (A-2), (A-3), we obtain the result as (13). This concludes our proof.

Appendix B: Proof of Lemma 3

Here, we derive the closed-form expression of Φ_s as follows.

$$\begin{aligned}\Phi_s &= \Pr\left(g_1 > g_2, \gamma_{11} > \gamma_{th}, \gamma_{12} > \gamma_{th}\right) + \Pr\left(g_1 < g_2, \gamma_{21} > \gamma_{th}, \gamma_{22} > \gamma_{th}\right) \\ &= \underbrace{\Pr\left(g_1 > g_2, \frac{a\gamma_0 g_1^2}{a\gamma_0 g_2^2 + 1} > \gamma_{th}, a\gamma_0 g_2^2 > \gamma_{th}\right)}_{I_3} \\ &+ \underbrace{\Pr\left(g_1 < g_2, a\gamma_0 g_1^2 > \gamma_{th}, \frac{a\gamma_0 g_2^2}{a\gamma_0 g_1^2 + 1} > \gamma_{th}\right)}_{I_4}\end{aligned} \tag{B-1}$$

$$\begin{aligned}I_3 &= \Pr\left(g_1 > g_2, g_1 > \sqrt{\gamma_{th}\left(g_2^2 + \frac{1}{a\gamma_0}\right)}, g_2 > \sqrt{\frac{\gamma_{th}}{a\gamma_0}}\right) \\ &= \begin{cases} \Pr\left(g_1 > \sqrt{\gamma_{th}\left(g_2^2 + \frac{1}{a\gamma_0}\right)}, g_2 > \sqrt{\frac{\gamma_{th}}{a\gamma_0}}\right), & \gamma_{th} > 1 \\ \Pr\left(g_1 > \sqrt{\gamma_{th}\left(g_2^2 + \frac{1}{a\gamma_0}\right)}, \sqrt{\frac{\gamma_{th}}{a\gamma_0(1-\gamma_{th})}} > g_2 > \sqrt{\frac{\gamma_{th}}{a\gamma_0}}\right) & \\ \qquad + \Pr\left(g_1 > g_2, g_2 > \sqrt{\frac{\gamma_{th}}{a\gamma_0(1-\gamma_{th})}}\right), & \gamma_{th} < 1 \end{cases}\end{aligned}$$

$$\stackrel{(c)}{=} \begin{cases} \frac{\pi}{N\lambda_2}\sum_{j=1}^{N}\exp\left(-\frac{\sqrt{\gamma_{th}\left(\theta_j^2 + \frac{1}{a\gamma_0}\right)}}{\lambda_1} - \frac{\theta_j}{\lambda_2}\right)\sqrt{\frac{1-\phi_j}{1+\phi_j}} & \\ \qquad -\frac{\pi b}{2N\lambda_2}\sum_{j=1}^{N}\exp\left(-\frac{\sqrt{\gamma_{th}\left(x_j^2 + \frac{1}{a\gamma_0}\right)}}{\lambda_1} - \frac{x_j}{\lambda_2}\right)\sqrt{1-\phi_j^2}, & \gamma_{th} > 1 \\ \frac{\pi(c-b)}{2N\lambda_2}\sum_{j=1}^{N}\exp\left(-\frac{\sqrt{\gamma_{th}\left(y_j^2 + \frac{1}{a\gamma_0}\right)}}{\lambda_1} - \frac{y_j}{\lambda_2}\right)\sqrt{1-\phi_j^2} & \\ \qquad + \frac{\lambda_1}{\lambda_1+\lambda_2}\exp\left[-\left(\frac{1}{\lambda_1} + \frac{1}{\lambda_2}\right)c\right], & \gamma_{th} < 1 \end{cases}. \tag{B-2}$$

where $b = \sqrt{\frac{\gamma_{th}}{a\gamma_0}}$, $c = \sqrt{\frac{\gamma_{th}}{a\gamma_0(1-\gamma_{th})}}$, step (c) is obtained by applying the Gaussian-Chebyshev quadrature method in which $\theta_j = -\ln\left(\frac{\phi_j+1}{2}\right)$, $x_j = \frac{(\phi_j+1)c}{2}$, $y_j = \frac{(\phi_j+1)(c-b)}{2} + b$, $\phi_j = \cos\left(\frac{2j-1}{2N}\pi\right)$, and N is the complexity-vs-accuracy trade-off coefficient.

Similarly, we obtain the expression of integral I_4 as follows:

$$I_4 = \begin{cases} \frac{\pi}{N\lambda_1}\sum_{j=1}^{N}\exp\left(-\frac{\sqrt{\gamma_{th}\left(\theta_j^2+\frac{1}{a\gamma_0}\right)}}{\lambda_2}-\frac{\theta_j}{\lambda_1}\right)\sqrt{\frac{1-\phi_j}{1+\phi_j}} \\ \qquad -\frac{\pi b}{2N\lambda_1}\sum_{j=1}^{N}\exp\left(-\frac{\sqrt{\gamma_{th}\left(x_j^2+\frac{1}{a\gamma_0}\right)}}{\lambda_2}-\frac{x_j}{\lambda_1}\right)\sqrt{1-\phi_j^2}, & \gamma_{th}>1 \\ \frac{\pi(c-b)}{2N\lambda_1}\sum_{j=1}^{N}\exp\left(-\frac{\sqrt{\gamma_{th}\left(y_j^2+\frac{1}{a\gamma_0}\right)}}{\lambda_2}-\frac{y_j}{\lambda_1}\right)\sqrt{1-\phi_j^2} \\ \qquad +\frac{\lambda_2}{\lambda_1+\lambda_2}\exp\left[-\left(\frac{1}{\lambda_1}+\frac{1}{\lambda_2}\right)c\right], & \gamma_{th}<1 \end{cases} \tag{B-3}$$

From (B-1), (B-2), (B-3), we obtain the result as (15). This concludes our proof.

References

1. Chettri, L., Bera, R.: A comprehensive survey on internet of things (IoT) toward 5G wireless systems. IEEE Internet Things J. **7**(1), 16–32 (2019)
2. Mao, Y., You, C., Zhang, J., Huang, K., Letaief, K.B.: A survey on mobile edge computing: the communication perspective. IEEE Commun. Surv. Tutor. **19**(4), 2322–2358 (2017)
3. Pham, Q.V., et al.: A survey of multi-access edge computing in 5G and beyond: fundamentals, technology integration, and state-of-the-art. IEEE Access **8**, 116974–117017 (2020)
4. Ye, Y., Lu, G., Hu, R.Q., Shi, L.: On the performance and optimization for MEC networks using uplink NOMA. In: IEEE International Conference on Communications Workshops (ICC Workshops), Shanghai, China. IEEE (2019)
5. Fang, F., Xu, Y., Ding, Z., Shen, C., Peng, M., Karagiannidis, G.K.: Optimal resource allocation for delay minimization in NOMA-MEC networks. IEEE Trans. Commun. **68**, 7867–7881 (2020)
6. Ha, D.-B., Truong, V.-T., Ha, D.-H.: A novel secure protocol for mobile edge computing network applied downlink NOMA. In: Vo, N.-S., Hoang, V.-P. (eds.) INISCOM 2020. LNICST, vol. 334, pp. 324–336. Springer, Cham (2020). https://doi.org/10.1007/978-3-030-63083-6_25
7. Ye, Y., Hu, R.Q., Lu, G., Shi, L.: Enhance latency-constrained computation in MEC networks using uplink NOMA. IEEE Trans. Commun. **68**(4), 2409–2425 (2020)
8. Min, M., et al.: Learning-based privacy-aware offloading for healthcare IoT with energy harvesting. IEEE Internet Things J. **6**(3), 4307–4316 (2018)
9. Zhou, F., Wu, Y., Hu, R.Q., Qian, Y.: Computation efficiency in a wireless-powered mobile edge computing network with NOMA. In: ICC 2019–2019 IEEE International Conference on Communications (ICC), pp. 1–7. IEEE (2019)
10. Hoang, T.M., Van Son, V., Dinh, N.C., Hiep, P.T.: Optimizing duration of energy harvesting for downlink NOMA full-duplex over Nakagami-m fading channel. AEU-Int. J. Electron. Commun. **95**, 199–206 (2018)

11. Garcia, C.E., Camana, M.R., Koo, I.: Particle swarm optimization-based secure computation efficiency maximization in a power beacon-assisted wireless-powered mobile edge computing NOMA system. Energies **13**(21), 5540 (2020). ISSN: 1996-1073
12. Ha, D.B., Tran, D.D., Tran-Ha, V., Hong, E.K.: Performance of amplify-and-forward relaying with wireless power transfer over dissimilar channels. Elektron. ir Elektrotechnika J. **21**(5), 90–95 (2015)
13. Zhou, F., Wu, Y., Hu, R.Q., Qian, Y.: Computation efficiency in a wireless-powered mobile edge computing network with NOMA. In: IEEE International Conference on Communications (ICC), Shanghai, China, pp. 20–24, May 2019
14. Guo, X., Su, J., Zhou, H., Liu, C., Cao, J., Li, L.: Community detection based on genetic algorithm using local structural similarity. IEEE Access **7**, 134583–134600 (2019)
15. Fang, P., Zhao, Y., Liu, Z., Gao, J., Chen, Z.: Resource allocation strategy for MEC system based on VM migration and RF energy harvesting. In: 2020 IEEE 91st Vehicular Technology Conference (VTC2020-Spring), pp. 1–6. IEEE (2020)
16. Hassanat, A., Almohammadi, K., Alkafaween, E., Abunawas, E., Hammouri, A., Prasath, V.: Choosing mutation and crossover ratios for genetic algorithms a review with a new dynamic approach. Information **10**(12), 390 (2019)
17. Chen, L., Wu, J., Long, X., Zhang, Z.: Engine: cost effective offloading in mobile edge computing with fog-cloud cooperation. arXiv preprint arXiv:1711.01683 (2017)
18. Truong, V.T., Vo, M.T., Lee, Y., Ha, D.B.: Amplify-and-forward relay transmission in uplink non-orthogonal multiple access networks. In: 2019 6th NAFOSTED Conference on Information and Computer Science (NICS), pp. 1–6. IEEE (2019)